

The Relation Between Melt Flow Properties and Molecular Weight of Polyethylene

SHIGERU SAEDA, JUNJI YOTSUYANAGI, and
KINYA YAMAGUCHI, *Central Research Laboratory,
Showa Denko, Co., Ltd., Ota-ku, Tokyo, Japan*

Synopsis

The non-Newtonian behavior of commercial linear polyethylene samples and their fractions were studied at 190°C. The viscosity η versus shear rate $\dot{\gamma}$ curves of whole polymers could be superimposed onto a single master curve despite the variations of their molecular weights and molecular weight distributions. For fractions, however, the same master curve was inapplicable, and the sensitivity of the viscosity to shear rate was found to be greater than those of the whole polymers. The zero-shear viscosities η_0 of fractions were related to the 3.42 power of the weight-average molecular weight M_w as follows:

$$\eta_0 = 2.39 \times 10^{-16} M_w^{3.42}.$$

For whole polymers, the zero-shear viscosities were found to be considerably higher at the same M_w and markedly lower at the same z -average molecular weight M_z than those of the fractions. Thus, it was concluded that η_0 corresponds to an average of molecular weight between M_w and M_z . It was found that the molecular relaxation time τ is proportional to $M_z^{5.3}$ for whole polymers and to $\eta_0 M_w$ for fractions. Using these relations it was possible to relate the flow ratio, the ratio of flow rates at two different shear stresses, with the molecular weight distribution.

INTRODUCTION

The non-Newtonian behavior of polymer melts has been one of the most important subjects in polymer science and technology. A great deal of experimental results has been accumulated¹ and a few theories have been presented as well. None of the present theories, however, seems to be perfect in describing the complicated behavior of the various polymer systems. It is our present purpose to establish experimentally correlations between the rheological parameters obtained from the non-Newtonian flow behavior and some molecular weight parameters.

According to Bueche,² who considered a single polymer chain, and Graessley,^{3,4} who postulated that two polymers can be entangled with each other when they approach within a limited distance, the reduced viscosity η/η_0 of the polymer is expressed as a function of shear rate $\dot{\gamma}$ and molecular relaxation time τ . It is important to note that the two theories concluded that η/η_0 should be a function of $\dot{\gamma}\tau$. In fact, both Bueche and Harding⁵

and Sabia⁶ showed experimentally that the $\log \eta$ versus $\log \dot{\gamma}$ relations can be superimposed onto a single master curve.

In this paper, attempts are made first to establish the master curves of viscosity for fractionated polyethylenes as well as commercial whole polymers over a wide range of molecular weights and molecular weight distributions, and to study the difference of the shape between them with the molecular weight distribution. Using the master curve, τ and η_0 are obtained as the shift factors. The molecular weight dependence of these rheological parameters will be discussed.

EXPERIMENTAL

Samples

The samples used in our experiments are listed in Tables I and II, together with their characterization data.

Samples of series A are the Phillips-type commercial linear polyethylenes with broad molecular weight distributions, and B samples are those with moderate molecular weight distributions. Samples C are the Phillips-type ethylene-butene copolymers with broad molecular weight distributions.

Samples F-1 to F-4 are fractions prepared from A-2 by column elution method. In this case, fractions from two parallel runs were combined to obtain large enough samples for the melt viscosity determinations. Samples F-5 to F-10 are fractions prepared from A-7 by a large-scale column fractionation technique. The molecular weight distributions of these fractions were confirmed to have $M_w/M_n = \text{ca. } 1.25$ and were sufficiently narrow compared with those of the whole polymers, as shown in Table II.

Fractionations and Molecular Weight Determinations

Ten samples were fractionated by column elution technique according to the method of Henry⁷ to determine the molecular weight distribution. Ethyl Cellosolve and xylene were used as the poor solvent and good solvent system, at 127°C. The molecular weights of the fractions were determined from the inherent viscosity according to the following empirical relation⁸ based on light scattering measurements:

$$\{\eta\} = 5.60 \times 10^{-4} M_w^{0.694} \quad \text{for fractions} \quad (1)$$

All the samples fractionated were found to have logarithmic normal distribution functions.⁹ The number-average molecular weight M_n , the weight average molecular weight M_w , and the z -average molecular weight M_z of the whole polymers which were fractionated were calculated from the summation method.

To get a large amount of fraction, 250 g of sample A-7 was fractionated by a large-scale column fractionation technique,¹⁰ in which a column with a length of 2 m and 10 cm in diameter was used. A system of butyl Cello-

TABLE I
 Characterization Data of Whole Polymers

Sample ^a	MI ^c	{ η } ^{1a}	$M_n^e \times 10^{-4}$	$M_w^f \times 10^{-4}$	$M_w^c \times 10^{-4}$	$M_z^c \times 10^{-4}$	M_w/M_n^e	η_0 , poise	τ , sec
A-1	0.92	1.81		12.8				5.3×10^5	1.4
A-2 ^b	0.94	1.88	1.36	13.5	14.4	61.3	10.6	6.8×10^5	2.6
A-3	3.44	1.42		8.99				1.0×10^5	1.5
A-4	5.0	1.36		8.55				9.1×10^4	4.9×10^{-1}
A-5 ^b	5.05	1.37	1.26	8.54	10.1	47.0	8.0	1.22×10^5	5.3×10^{-1}
A-6	5.82	1.30		7.92				6.0×10^4	3.6×10^{-1}
A-7	3.0	1.45		8.23				—	—
B-1 ^b	3.00	1.54	1.80	10.1	10.1	36.7	5.61	1.03×10^5	1.4×10^{-1}
B-2	4.64	1.36		8.40				5.8×10^4	8.3×10^{-2}
B-3 ^b	7.96	1.22	1.87	7.21	7.33	22.0	3.92	3.2×10^4	2.6×10^{-2}
B-4	10.4	1.17		6.79				2.0×10^4	1.8×10^{-2}
B-5 ^b	15.5	1.05	1.56	5.80	6.43	22.2	4.12	1.3×10^4	9.8×10^{-3}
B-6 ^b	15.7	1.12	1.50	6.37	6.37	19.1	4.26	1.0×10^4	5.3×10^{-3}
B-7 ^b		1.10	1.53	6.20	6.60	23.5	4.32	1.5×10^4	1.7×10^{-2}
C-1 ^b	0.36	2.36	1.12	18.8	21.0	83.1	18.8	2.8×10^6	1.7×10
C-2	0.35	2.40		19.3				3.9×10^6	3.0×10
C-3	3.24	1.47		9.45				1.5×10^5	8.3×10^{-1}
C-4	0.89	1.83		13.0				8.8×10^5	6.0
C-5	6.24	1.27		7.66				7.8×10^4	3.2×10^{-1}
C-6 ^b		1.33	1.33	8.18	8.75	40.9	6.6	8.0×10^4	3.3×10^{-1}
C-7		1.32		8.10				8.0×10^4	2.1×10^{-1}
C-8 ^b		1.28	0.81	7.73	8.57	46.7	10.6	1.17×10^5	6.7×10^{-1}

^a A, Linear PE with broad MWD; B, linear PE with moderate MWD; C, ethylene-butene copolymer with broad MWD, with 1-2 CH₃/1000 C. The values of M_w from light scattering of A-2, A-3, and A-5 were 12.7×10^4 , 8.93×10^4 , and 8.06×10^4 , respectively.

^b Fractionated samples.

^c ASTM D1238-57T.

^d Measured in tetralin at 130°C, 0.1% concentration.

^e Calculated from fractionation data by summation method.

^f From { η } with eq. (2).

TABLE II
 Characterization Data of Fractions

Sample ^a	$\{\eta\}^b$	$M_w^c \times 10^{-4}$	$M_n^d \times 10^{-4}$	M_w/M_n	η_0 , poise
F-1	0.523	1.92			1.15×10^2
F-2	1.09	5.38			3.9×10^3
F-3	1.62	9.73			2.95×10^4
F-4	6.53	72.4			2.55×10^4
F-5	0.228	0.604	0.495	1.22	2.29
F-6	0.482	1.74	1.40	1.24	6.71×10
F-7	0.943	4.47	3.58	1.25	2.80×10^3
F-8	1.36	7.51	5.92	1.29	1.35×10^4
F-9	2.55	18.2	14.7	1.29	1.90×10^5
F-10	4.79	44.0			9.10×10^{6a}

^a F-1 to F-4 are fractions from A-2; F-5 to F-10 are fractions from A-7. The values of M_n from osmotic pressure of F-7, F-8, and F-9 were 3.59×10^4 , 5.82×10^4 , and 14.1×10^4 , respectively. Samples F-1 to F-6 were measured by a cone-and-plate viscometer, samples F-7 to F-10 by an extrusion rheometer.

^b Measured in tetralin at 130°C, 0.1% concentration.

^c From $\{\eta\}$ with eq. (1).

^d From vinyl unsaturation.

^e Extrapolated value.

solve and xylene was used at 125°C in this case. The values of M_w from inherent viscosities and those of M_n wherever possible from infrared measurements of terminal vinyl unsaturation¹¹ are indicated in Table II. The values of M_n from the infrared method showed an excellent agreement with those from osmotic pressure measurement, as indicated in the footnote of Table II.

For whole polymers, the following empirical relation established before⁸ between $\{\eta\}$ and M_w from light scattering was employed in estimating the viscosity-average molecular weight M_v :

$$\{\eta\} = 5.48 \times 10^{-4} M_w^{0.689} \quad \text{for whole polymers} \quad (2)$$

The values of M_v from inherent viscosities are not much different from M_w from direct measurement of light scattering for whole polymers, as indicated for some samples in the footnote of Table I. Therefore, in this paper the values of M_v are treated as M_w .

Measurements of light scattering were performed by a Shimadzu light-scattering photometer PG-21, in α -chloronaphthalene at 125°C, while M_n values were measured with a membrane osmometer Model 501 produced by Hewlett-Packard, in Tetralin at 130°C. The inherent viscosities were measured at 130°C in Tetralin at about 0.1% concentration, with a Cannon-Fenske-type viscometer.

Melt Viscosity

Most experiments were performed with a cone-and-plate-type viscometer, Model V-1205A, manufactured by Rion Co., Ltd. Both cone and plate are set in a small electric furnace equipped with a Thermistor tem-

perature-regulating system. The angular velocity ω was measured while a given torque M was applied to the lower plate, in keeping the upper cone at a fixed position. The viscosity η , the shear stress S , and the shear rate $\dot{\gamma}$ were calculated by the following relations:

$$S = 3M/2\pi R^3 \quad (3)$$

$$\dot{\gamma} = \omega/\theta \quad (4)$$

$$\eta = S/\dot{\gamma} \quad (5)$$

where θ is the angle between the cone and the plate and R is the radius of the plate. A cone and plate set with $R = 6$ cm and $\theta = 5^\circ$ was mainly used. The other sets such as those with $R = 6$ cm and $\theta = 2^\circ$ or with $R = 3$ cm and $\theta = 5^\circ$ were also used in a few cases. Viscosities from each cone and plate set agreed with each other within the experimental error.

All the measurements were carried out at a temperature of 190°C . The correction for edge effect was not applied, because it causes no serious error in this type of viscometer.

A gas-operated extrusion-type viscometer, Takara Flow Tester Model FT-203, was also used in some cases to measure the viscosity at higher range of shear rate. Shear stress and shear rate were calculated by the familiar relation as follows:

$$S = PR/2L \quad (6)$$

$$\dot{\gamma} = 4Q/\pi R^3 \quad (7)$$

where P is the applied pressure, Q is the volumetric flow rate, and R and L are the radius and length of the capillary, respectively. The capillary end correction according to Bagley¹² and the Rabinowitsch correction¹³ were applied for whole polymers. A series of capillaries 0.489 mm in diameter and with length-to-diameter ratios of 5, 10, and 15 were used in this case.

For fractions, a capillary 1.092 mm in diameter and with a length of 32.76 mm was used without corrections.

RESULTS AND DISCUSSION

Master Curve

The variation in viscosity η with shear rate $\dot{\gamma}$ is illustrated in Figure 1 for several whole polymers, i.e., A-2, B-1, and C-1. As expected, the viscosity increases as the molecular weight becomes larger. The slope of each curve at the same shear rate, which is taken as a measure of the non-Newtonian behavior, also increases with the molecular weight. Both viscosity data obtained by a cone-and-plate viscometer and a gas-operated extrusion-type viscometer are included in the same figure. It is interesting to note that the viscosity-shear rate relations derived by these two different

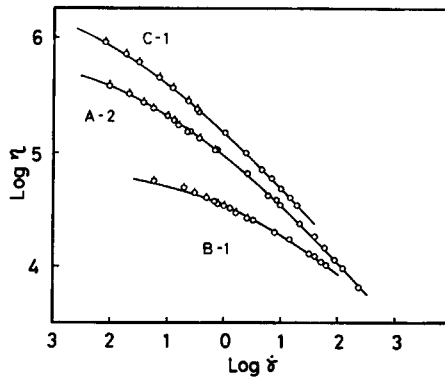


Fig. 1. The variation of viscosity with shear rate for whole polymers at 190°C: (⊙) measured by cone-and-plate viscometer; (○) measured by extrusion rheometer.

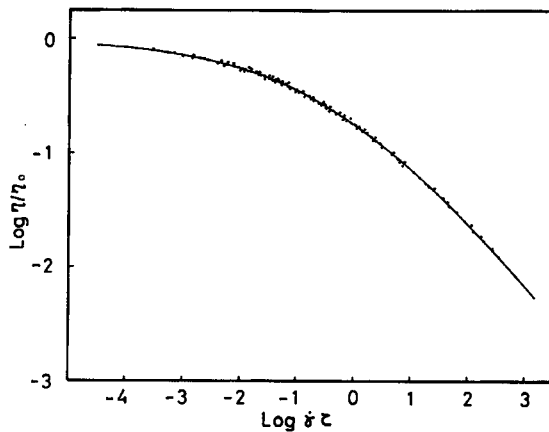


Fig. 2. Viscosity master curve of whole polymers.

methods in the low shear and in the high shear regions, respectively, lie on a single smooth curve for a given polymer sample. Although these are not shown in the figure, viscosities of samples B-5 and C-8 were also measured by the two viscometers for about four decades of shear rate. The other whole polymers were measured by a cone-and-plate viscometer.

Following the method of Bueche and Harding⁵ and Sabia,⁶ the observed $\log \eta$ versus $\log \dot{\gamma}$ relations of commercial whole polymers were superimposed with some appropriate shifting along each axis. Within the experimental error, a composite master curve was obtained as shown in Figure 2. The relation can be represented satisfactorily by the following equation, of the same type as that used by Sabia⁶:

$$\log (\eta/\eta_0) = [(\eta/\eta_0) - 8/3] \log [1 + (\dot{\gamma}\tau)^{1/4}] \quad (8)$$

The situation is rather different for the fractionated polymers. In Figure 3, the results obtained for the fractions in the F series are shown.

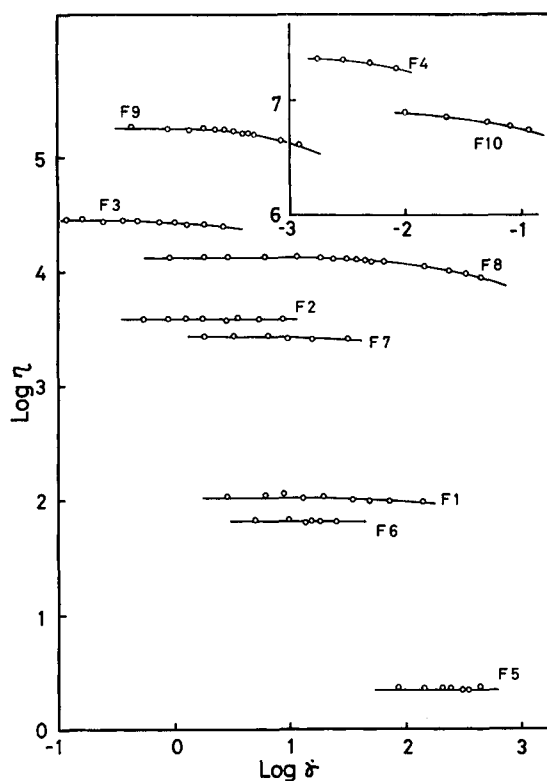


Fig. 3. Variation of viscosity with shear rate for fractions at 190°C.

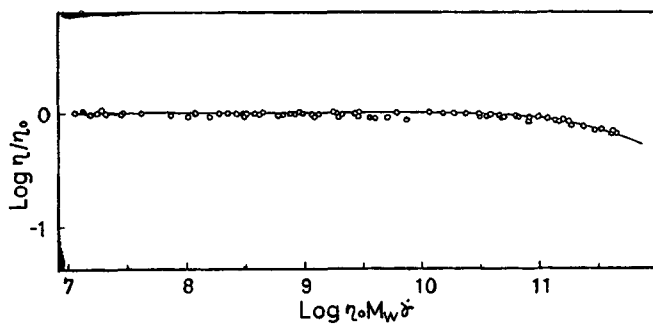


Fig. 4. Viscosity master curve of fractions.

Their viscosities reach easily to their Newtonian region in the measurable shear rate range, in contrast to the curves of the whole polymers shown in Figure 1. The weight-average molecular weights of samples F-3 and B-1 are 9.73×10^4 and 10.1×10^4 , respectively, being almost identical with each other. Nevertheless, these two samples differ very much in their flow behavior: while B-1 shows quite a drastic non-Newtonian flow, that of F-3 is approximately Newtonian.

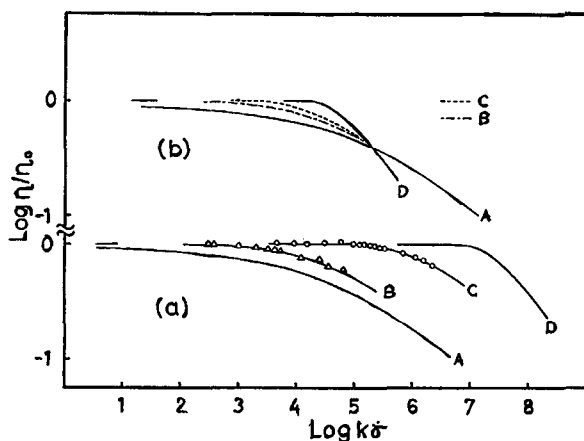


Fig. 5. Sensitivity of viscosity to shear rate with various molecular weight distributions. Abscissa is shifted arbitrarily for the convenience of drawing. (a): A, Master curve for whole polymers; B, fraction with $M_w = 5.5 \times 10^4$, $M_w/M_n = 1.9$, from data of Schreiber¹⁶; C, master curve of fractions with $M_w/M_n = \text{ca. } 1.25$, with plots of F-8; D, monodisperse polystyrene.^{14,15} (b): Curves of (a) shifted horizontally to their closest approach to clarify their difference in shapes.

The superposition of flow curves was also possible for fractions as for whole polymers. A reduced flow curve was obtained by plotting the data in the form η/η_0 versus $\eta_0 M_w \dot{\gamma}$, as shown in Figure 4. This means that the shift factor τ is proportional to $\eta_0 M_w$ in accordance with the results of Ballman and Simon¹⁴ and Wyman, Elyash, and Frazer¹⁵ for monodisperse polystyrenes. At the same time, this supports the theoretical prediction of Bueche² and Graessley.^{3,4} However, we must note the limitation of Figure 4 that the range of η/η_0 is very small. This is due to the fact that the polyethylene fractions easily break into the melt fracture region at low shear rates and in the proximity of the Newtonian region.

Comparing the two master curves for whole polymers and fractions, it is interesting to note here that the shapes of the two master curves are considerably different from each other, as clearly indicated in Figure 5. The sensitivity of the viscosity with shear rate for the fractions is greater than for the whole polymers. The same phenomena were already observed for polydisperse and anionically polymerized nondisperse polystyrenes.^{14,15}

The data of Schreiber¹⁶ on linear polyethylene fractions with $M_w = 5.5 \times 10^4$ and $M_w/M_n = 1.9$, which were prepared by a large-scale cocervation method, are also indicated in Figure 5. It is interesting to note that the viscosities of his fraction are less sensitive to the shear rate than our fractions, having narrower molecular weight distributions of $M_w/M_n = \text{ca. } 1.25$. The sensitivity of our fractions, on the other hand, is smaller than that of the monodisperse polystyrene,^{14,15} which was in accordance with the theoretical curve for monodisperse polymers proposed by Graessley.⁴

It is concluded, therefore, that the shape of the flow curves changes considerably with the sharpness of the molecular weight distribution for polyethylenes, especially in the range of narrow molecular weight distributions.

In cases of commercial linear polyethylenes with M_w/M_n greater than about 4, however, the effect of molecular weight distribution on the shape of the flow curves seems very small, as shown in Figure 2. The results are in agreement with the calculation of Graessley⁴ in that the change of the shape of the flow curves with molecular weight distribution is large in the range of molecular weight distributions close to monodisperse, and gradually becomes smaller as the distribution broadens. In fact, the theoretical flow curves derived from Graessley's theory for some whole polymers shown in Table I were found to be almost the same.¹⁷ Thus, eq. (8) can be used in practice for ordinary commercial linear polyethylenes.

The values of η_0 and τ for whole polymers obtained from the above eq. (8) are listed in Table I.

The values of η_0 of the fractions were obtained directly from their Newtonian region. In the case of F-4 and F-10, where the viscosities did not reach to their Newtonian region, η_0 values were obtained by use of the following empirical relation of Spencer and Dillon¹⁸:

$$1/\eta = 1/\eta_0 + KS \quad (9)$$

where K is a constant.

Zero Shear Viscosities of Fractions

The zero shear viscosities of the fractions are plotted against the weight-average molecular weights in Figure 6. Both the ordinate and abscissa are arranged in the logarithmic scale. The plots of ten fractions studied lies on a straight line with a slope of 3.42, which is very close to the theoretical value of 3.5, as shown in the figure. The straight line can be expressed by the following equation.

$$\eta_0 = 2.39 \times 10^{-5} M_w^{3.42} \quad (10)$$

Schreiber, Bagley, and West¹⁹ have already studied the relation between η_0 and M_w for fractions of Phillips-type linear polyethylene prepared by a large-scale coacervation method. Their results are also shown in the same figure. In the region of low molecular weight the discrepancy is small, but at higher molecular weights, their viscosities are considerably higher than the present results, which produced their higher exponent of 4.10. This disagreement may be due to the fact that their fractions show a dependence of polydispersity on molecular weight. As Blackmore and Alexander²⁰ indicated, the fractions from the large-scale coacervation method have very high values of M_w/M_n (ca. 8 for the highest molecular weight fraction) at high molecular weight, though gradually the value becomes smaller with decreasing molecular weight. This seems to be the reason for their

higher exponent, because the broader the molecular weight distribution, the higher become the zero-shear viscosities at the same M_w , as will be shown in the later section. Our fractions obtained from the column elution method have very narrow molecular weight distribution ($M_w/M_n = \text{ca. } 1.25$), and the distributions have no serious molecular weight dependence, as shown in Table II.

The data of Tung²¹ for Ziegler-type polyethylene fractions prepared by a coacervation and an elution method are also shown in Figure 6. The viscosities are about half a decade greater than ours, although the slope

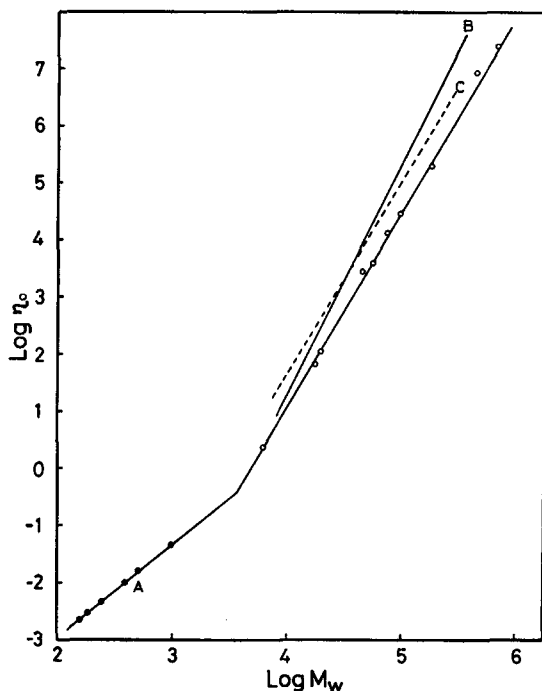


Fig. 6. Zero-shear viscosities of fractions vs. M_w at 190°C: A, *n*-alkane, data of Doolittle²³; B, data of Schreiber and co-workers¹⁹; C, data of Tung.²¹

is almost the same. The reason for the disagreement in viscosities is not clear at present, because he did not state clearly the polydispersity of his fractions. But the fact that his viscosities of fractions at 150°C agreed with those of the whole polymers of Peticolas and Watkins²² at the same temperature suggests that the molecular weight distribution of their fractions might be broader than ours. In addition, if his fractions have long-chain branches as suggested in his paper, the direct comparison to our linear fractions is inappropriate.

With the viscosity data of *n*-alkanes of Doolittle,²³ the entanglement molecular weight M_c of polyethylene at 190°C can be obtained from the intersection of the relationships for *n*-alkane and linear polyethylene frac-

tions, as shown in Figure 6. The value thus obtained was $M_c = 3375$, which is rather lower than that obtained by Schreiber and co-workers.¹⁹

Zero-Shear Viscosities of Whole Polymers

The zero-shear viscosity data of whole polymers are plotted against M_w values in Figure 7. There is a clear trend that the sharper the molecular weight distribution, the smaller is the η_0 at a given value of M_w , in agreement with the result of McGlamery and Harban.²⁴ The samples of the F series with a molecular weight distribution of $M_w/M_n \cong 1.25$ fall on the lowest line in the figure. The second lowest line corresponds to the samples with $M_w/M_n = 4\sim 5$, which are chosen from the B series. Samples of the A and C series fall on the highest line. The molecular weight distribution of the A and C series was found to be $7\sim 19$ in terms of M_w/M_n . These experimental observations imply that the η_0 is related to some higher average molecular weight than M_w .

The M_w values of whole polymers in Figure 7 were obtained from the experimental relationship between intrinsic viscosity and M_w from light scattering, eq. (2), which is known to be dependent on the molecular weight distribution. In Table I, the M_w values calculated from fractionation data by summation method and direct measurement of light scattering are also shown wherever possible. The M_w values from these three sources agree with each other within about 10%. Hence the results in Figure 7 would hold true if all the samples were measured by light scattering.

The samples of the C series have 1-2 ethyl branches per 1000 carbon atoms. As shown in Figure 7 and in the following figures, the C polymers do not deviate from the A polymers. Thus, it is concluded that a few ethyl branches in polyethylenes have no appreciable effect on melt behavior, as pointed out by Schreiber.²⁵

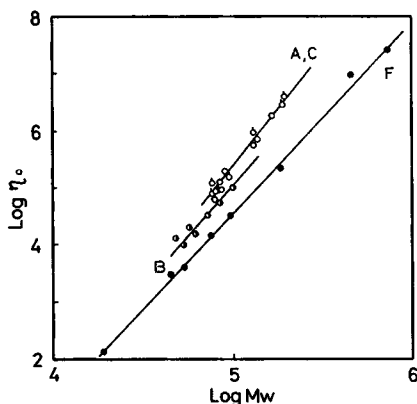


Fig. 7. Zero-shear viscosities of polyethylenes vs. M_w with different molecular weight distributions at 190°C: A, C, broad MWD; B, moderate MWD; F, fractions.

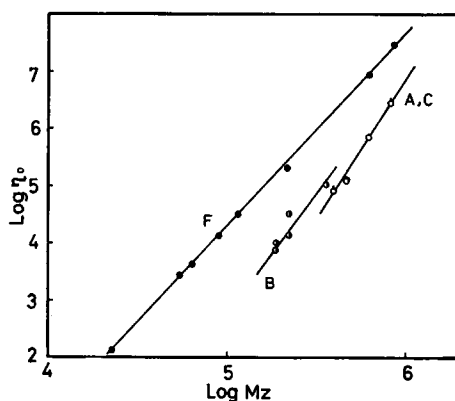


Fig. 8. Zero-shear viscosities of polyethylenes vs. M_z with different molecular weight distributions at 190°C: A,C, broad MWD; B, moderate MWD; F, fractions.

The two straight lines drawn in Figure 7 give us the following empirical η_0 versus M_w relations for samples with moderate molecular weight distributions (B) and those with broad molecular weight distributions (A,C):

$$\eta_0 = 1.20 \times 10^{-14} M_w^{3.78} \quad \text{for B} \quad (11)$$

$$\eta_0 = 3.02 \times 10^{-15} M_w^{3.97} \quad \text{for A,C} \quad (12)$$

The so-called 3.4 exponent rule holds only for the fractionated samples. The higher exponents for the two whole-polymer series apparently are attributable to the fact that the molecular weight distribution widens in general as the molecular weight itself increases.²⁶

The dependence of η_0 on the z -average molecular weight M_z was also studied. The $\log \eta_0$ versus $\log M_z$ relations for some linear polymers are shown in Figure 8. The M_z values of the whole polymers were determined from their fractionation data by the summation method. Those of the fractionations were obtained with the relation $M_z/M_w = M_w/M_n$ (assuming the average value of M_w/M_n to be 1.25), which holds for the log normal distribution of molecular weight, since the fractionation of a fraction obtained by column elution method showed that its distribution function was also a log normal type as its mother polymer.²⁷ The relative positions among the aforementioned three groups of linear polyethylenes are reversed, as compared with those in Figure 7. This undoubtedly indicates that the zero-shear viscosity η_0 can be related to an average molecular weight between M_w and M_z .

Fox and Flory²⁸ and Fox and Allen²⁹ have presented the following relation between η_0 and M_w for polyisobutylene and polystyrene systems:

$$\eta_0 = K M_w^{3.4} \quad K = \text{const.} \quad (13)$$

The same rule is apparently inapplicable to the polyethylene systems with very broad molecular weight distributions.

Our experimental results seem to support the proposal of Bueche³⁰ and Graessley⁴ that the zero shear viscosity is related to some average molecular weight M_t according to the following relation:

$$\eta_0 = K' M_t^{3.4} \quad K' = \text{const.} \quad (14)$$

where $M_w < M_t < M_z$. The M_t is much closer to M_w when the molecular weight distribution is narrow and approaches M_z as the molecular weight distribution widens.

Molecular Relaxation Time

The relation of τ and η_0 is shown in a double-logarithmic scale in Figure 9. The values of τ of group B with moderate molecular weight distributions still remain in the region below those of A or C with broader molecular

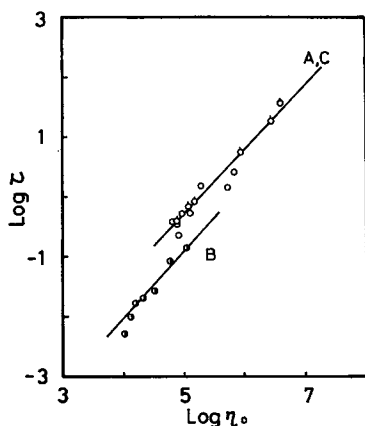


Fig. 9. Molecular relaxation times of polyethylenes with different molecular weight distributions vs. zero-shear viscosity at 190°C: A,C, broad MWD; B, moderate MWD.

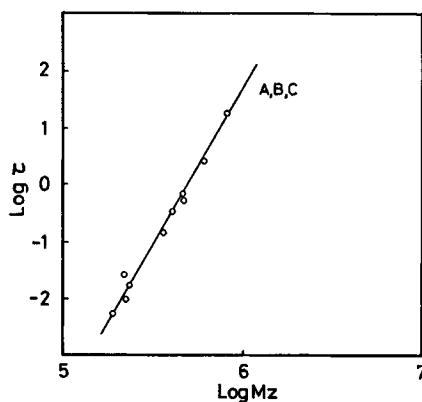


Fig. 10. Molecular relaxation times vs. M_z for polyethylenes with different molecular weight distributions at 190°C: A,C, broad MWD; B, moderate MWD.

weight distributions. This leads us to the conclusion that the molecular relaxation time relates to a molecular weight of higher moment than that for η_0 .

The relation of $\log \tau$ versus $\log M_z$ is shown in Figure 10, where all samples of the A, B, and C series can be arranged on a single straight line. In the range of the molecular weight distributions studied, the molecular relaxation time τ can be best represented by the following equation:

$$\tau = 5.59 \times 10^{-31} M_z^{5.30} \quad (15)$$

This result means that the flow curves of whole polymers are shifted proportional to the 5.3 power of M_z along the abscissa. Although there is no theoretical background to explain the results at the present time, it is interesting to compare them with the result of fractions that show that the shift factor τ is proportional to $\eta_0 M_w$ or to $M_w^{4.42}$ using eq. (10).

Flow Ratio

The flow ratio, the ratio of two flow rates at high and low shear stresses obtained by an extrusion-type rheometer, is often used as a practical measure of the molecular weight distribution. Some experimental efforts were made to relate the flow ratio and the parameter of molecular weight distribution. However the results are not in agreement with each other. Martinovitch and co-workers³¹ showed that the flow ratio is linearly related to M_w/M_n ; on the other hand, Cottam³² claimed a linear relation of flow ratio and M_z . Sakamoto³³ obtained a linear relation for the logarithm of flow ratio and M_z/M_w .

Our result shown in Figure 10 and eq. (15), together with the master curve, can be used to have a further insight into the flow ratio.

When the master curve of the whole polymer, eq. (8), is rewritten in terms of shear stress S , using the relation $\eta = S/\dot{\gamma}$, we can easily obtain the following:

$$\log (\eta/\eta_0) = [(\eta/\eta_0) - 3/3] \log [1 + (\eta_0/\eta)^{1/4} (\tau/\eta_0 \cdot S)^{1/4}]. \quad (16)$$

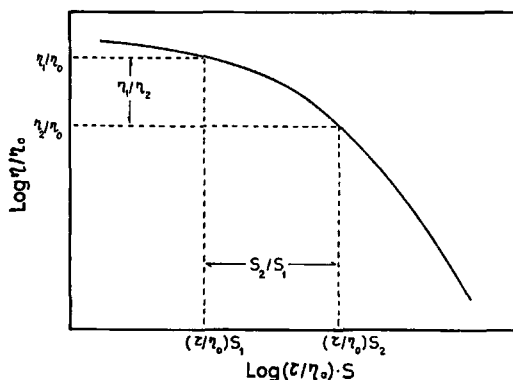


Fig. 11. Schematically drawn viscosity master curve in terms of shear stress.

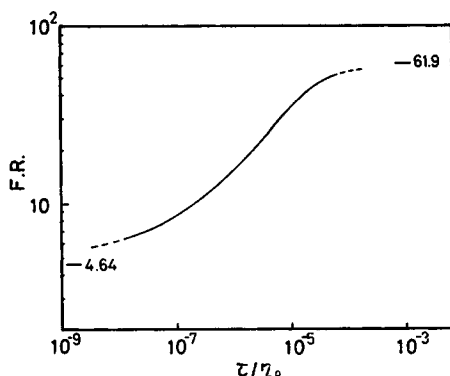


Fig. 12. Variation of flow ratio $F.R.$ with τ/η_0 in the case of melt indexer, with 2.16 kg and 10 kg weights. Values of 4.64 and 61.9 indicate minimum and maximum flow ratios, respectively.

Here it must be noted that now τ/η_0 , instead of τ in eq. (8), is the shift factor of the abscissa. If two flow rates are denoted as Q_1 and Q_2 at arbitrarily chosen pressures P_1 and P_2 , the flow ratio $F.R.$ is

$$F.R. = Q_1/Q_2; \quad (17)$$

and when the same capillary is assumed, from eq. (6) and eq. (7),

$$F.R. = (S_2/S_1)(\eta_1/\eta_2) = (P_2/P_1)(\eta_1/\eta_2). \quad (18)$$

Because S_1 and S_2 are known, we can obtain the η_1/η_2 values from arbitrarily chosen τ/η_0 values and the master curve based on shear stress, eq. 16, as shown schematically in Figure 11. We can thus obtain pairs of $F.R.$ and τ/η_0 from eq. (18). The relation between $\log F.R.$ and $\log \tau/\eta_0$ is shown in Figure 12 for the case of a melt indexer where the weights were chosen as 2.16 and 10 kg, respectively.

From the master curve it can be expected that $F.R.$ remains constant in the Newtonian region because the viscosity does not change with shear stress. At very high values of τ/η_0 , η_1/η_2 becomes constant because the slope of the master curve approaches a straight line, so that the $F.R.$ value also becomes constant. The important region for practical interest lies between the above two extremes. There is a region where $\log F.R.$ versus $\log \tau/\eta_0$ is approximated by a straight line. The equation for it may be written as:

$$F.R. = K_1(\tau/\eta_0)^\alpha \quad K_1, \alpha = \text{const.} \quad (19)$$

Combining eq. (19) with eqs. (14) and (15), we obtain

$$F.R. = K_2(M_z^{5.3}/M_t^{3.4})^\alpha \quad K_2, \alpha = \text{const.} \quad (20)$$

This implies that the flow ratio is related to a factor of molecular weight distribution ($M_z^{5.3}/M_t^{3.4}$) that is particularly sensitive to the high molecular weight fraction of polymers. This result is close to that of Sakamoto.

It must be noted here that because eq. (15) holds only for whole polymers with moderate and broad molecular weight distributions, eq. (20) is only applicable to the polymers of the same range of molecular weight distribution, i.e., $M_w/M_n = 4-19$.

In the case of fractions, however, the situation is rather different. As shown in the earlier section, the superposition of flow curves of fractions were attained by setting $\tau = \eta_0 M_w$. In this case, the *F.R.* value must be a function of M_w only instead of M_z and M_i in eq. (20). If the master curve for monodisperse polymer is established, the flow ratio can be used to estimate the molecular weight instead of the molecular weight distribution.

References

1. V. Semjonov, *Advan. Polym. Sci.*, **5**, 387 (1968).
2. F. Bueche, *J. Chem. Phys.*, **22**, 1570 (1954); *idem.*, *Physical Properties of Polymers*, Interscience, New York, 1962.
3. W. W. Graessley, *J. Chem. Phys.*, **43**, 2696 (1965).
4. W. W. Graessley, *J. Chem. Phys.*, **47**, 1942 (1967).
5. F. Bueche and S. W. Harding, *J. Polym. Sci.*, **32**, 177 (1958).
6. R. W. R. Sabia, *J. Appl. Polym. Sci.*, **7**, 347 (1963).
7. P. M. Henry, *J. Polym. Sci.*, **36**, 3 (1959).
8. K. Yamaguchi, unpublished data.
9. H. Wesslau, *Makromol. Chem.*, **20**, 111 (1956).
10. S. Saeda and K. Yamaguchi, to be published; A. S. Kenyon, I. O. Salyer, J. E. Kurz, and D. R. Brown, *J. Polym. Sci.*, **C-8**, 205 (1965).
11. D. C. Smith, *Ind. Eng. Chem.*, **48**, 1161 (1956).
12. E. B. Bagley, *J. Appl. Phys.*, **28**, 624 (1957).
13. B. Rabinowitsch, *Z. Phys. Chem.*, **A145**, 1 (1929).
14. R. L. Ballman and R. H. M. Simon, *J. Polym. Sci.*, **A-2**, 3557 (1964).
15. D. P. Wyman, L. J. Elyash, and W. J. Frazer, *J. Polym. Sci.*, **A-3**, 681 (1965).
16. H. P. Schreiber, *J. Appl. Polym. Sci.*, **9**, 2101 (1965).
17. S. Saeda, K. Yamaguchi, and T. Suzuki, *Zairyo*, **19**, 306 (1970).
18. R. S. Spencer and R. E. Dillon, *J. Colloid Sci.*, **4**, 241 (1949).
19. H. P. Schreiber, E. B. Bagley, and D. C. West, *Polymer*, **4**, 355 (1963).
20. W. R. Blackmore and W. Alexander, *Can. J. Chem.*, **39**, 1888 (1961).
21. L. H. Tung, *J. Polym. Sci.*, **46**, 490 (1960).
22. W. Peticolas and J. M. Watkins, *J. Amer. Chem. Soc.*, **79**, 5083 (1957).
23. A. K. Doolittle, *J. Appl. Phys.*, **22**, 1031 (1951).
24. R. M. McGlamery and A. A. Harban, *Mater. Res. Stand.*, **3**, 1003 (1963).
25. H. P. Schreiber, E. B. Bagley, *J. Polym. Sci.*, **58**, 29 (1962).
26. R. N. Howard, B. Wright, G. R. Williamson, and G. Thackray, *J. Polym. Sci.*, **A-2**, 2977 (1964).
27. K. Yamaguchi, unpublished data.
28. T. G. Fox and P. J. Flory, *J. Amer. Chem. Soc.*, **70**, 2384 (1948).
29. T. G. Fox and V. R. Allen, *J. Chem. Phys.*, **41**, 337 (1964).
30. F. Bueche, *J. Polym. Sci.*, **43**, 527 (1960).
31. R. J. Martinovitch, P. J. Boeke, and R. A. McCord, *SPE J.*, **16** 1335 (1960).
32. B. J. Cottam, *J. Appl. Polym. Sci.*, **9**, 1853 (1965).
33. H. Sakamoto, K. Kataoka, Y. Fukasawa, and H. Funahashi, *Zairyo*, **15**, 377 (1966).

Received June 1, 1970

Revised July 2, 1970